Fragility-Based Analysis for Joint Transmission and Generation Outages Under Hurricane Hazards

Maedeh Mahzarnia
Dept. of Electrical & Computer Engineering
Texas A&M University
College Station, TX, USA
maedehmahzarnia@tamu.edu

Farnaz Safdarian
Dept. of Electrical & Computer Engineering
Texas A&M University
College Station, TX, USA
fsafdarian@tamu.edu

Jonathan M. Snodgrass
Dept. of Electrical & Computer Engineering
Texas A&M University
College Station, TX, USA
snodgrass@tamu.edu

Thomas J. Overbye
Dept. of Electrical & Computer Engineering
Texas A&M University
College Station, TX, USA
overbye@tamu.edu

Abstract—This paper develops a fragility-based seasonal framework for probabilistic outage scenario generation under hurricane wind hazards. Wind exposure from nearby weather stations is assigned to transmission lines and generators using maximum seasonal wind gust, converted to m/s for asset-dependent lognormal fragility evaluation. Resulting outage probabilities generate seasonal transmission-only, generation-only, and joint transmission-generation Monte Carlo scenario sets with explicit probabilities; each 10,000-scenario ensemble is reduced through clustering to a representative probability-preserving subset. Applied to the Texas 7k synthetic grid using 2025 wind data, fall produces the largest transmission burden, averaging 3,591 failed lines, while joint line-generator outage probability is highest in spring and winter at 0.87 and 0.71, respectively, with negligible generator failures in summer. The joint outage space is therefore line-dominated in failed-asset count but generator-sensitive in participation probability, while the reduced probability-weighted libraries preserve dominant outage burden for downstream contingency and resilience studies.

Index Terms—Hurricane Resilience, Fragility-based Outage Modeling, Joint Outage Scenarios, Monte Carlo Simulation, Scenario Reduction.

I. INTRODUCTION

Extreme weather poses major threats to power-system reliability, and hurricanes are among the most complex hazards to model because they can be fast-moving and widespread. In hurricane-prone regions, the resulting system stress is not limited to a single operating condition or a single asset class. Hurricane-driven outages can simultaneously degrade network transfer capability and local generation availability by impacting both transmission and generation assets. Meaningful analysis requires a probabilistic representation of how hurricane-driven outages appear across the system.

References [1]–[4] examine hurricane risk through transmission fragility modeling, outage forecasting, and post-event restoration analysis. Fragility-based formulations are particularly useful because they relate failure probability directly to hazard intensity rather than to broad weather states, and they have been used to evaluate energy not supplied, outage cost, and asset damage for hurricane-exposed transmission networks [1], [3]. Predictive outage analytics have likewise been applied to estimate outage counts, duration, and restoration time for storm preparation [2], [5]. Distribution-side spatiotemporal risk analysis has recently been validated against real outage data from Hurricane Fiona [6], and coupled climate–energy modeling has begun to integrate renewable-resource vulnerability into cascading outage simulation [7]. Complementary efforts integrate weather and other resiliency hazards directly into power-flow modeling for transmission planning [8], including extensible formulations for representing deterministic and stochastic external inputs in the power flow [9]. Generation-side modeling remains comparatively limited: solar PV hurricane vulnerability has been characterized through coupled hazard, panel-failure, and irradiance-decay models [10], but other generator classes are typically simplified or implicitly assumed to remain available unless disconnected by network outages. Scenario-reduction methods are well established for power-system stochastic optimization, ranging from classical clustering-based selection [11] to more recent problem-driven reduction [12] and earlier transmission-line-only resilience workflows [13]. Hurricane case studies on the Texas synthetic grid have also been presented in [14].

Despite the current literature, several limitations persist. First, independent transmission outage studies can underestimate disruption when local generation availability is degraded. This can overlook the fact that available supply may still be constrained by a damaged network, and may miss outage states whose structure is not recoverable from separate treatment of the two asset classes. Second, temporal representation is similarly constrained, since many studies are organized around a single historical, simulated, or forecast storm rather than around seasonal variation in exposure and vulnerability [15]. Collectively, these efforts provide important building blocks, but few studies combine seasonal hazard characterization, asset-specific transmission-line and generator fragility, explicit joint outage-probability construction, and probability-preserving reduction for large synthetic grids.

To address these limitations, we develop a fragility-based seasonal framework for probabilistic outage scenario generation under hurricane wind hazards. We estimate outage probabilities for both transmission lines and generators using component-specific wind exposure together with asset-type-dependent fragility models. We construct seasonal scenario sets for transmission-only, generation-only, and joint transmission-generation outages with explicit scenario probabilities and reduce the full Monte Carlo ensembles to representative probability-preserving subsets through clustering-based

This work is part of the "Electric Grid Resilience" Project (60NANB24D210) funded by the National Institute of Standards and Technology of US Department of Commerce. The views expressed herein do not necessarily represent the views of the U.S. Department of Energy or the United States Government.

Copyright ©2026 IEEE. Personal use of this material is permitted. North American Power Symposium (NAPS) 2026, Houghton, MI, October 2026.

reduction. We demonstrate the framework on the Texas 7k synthetic grid. The main contributions of this paper are:

- a seasonal fragility-based outage modeling framework for both transmission branches and generators under hurricane wind hazards
- a unified scenario-generation formulation for transmission-only, generation-only, and combined line-generator outage classes with explicit scenario probabilities
- a probability-preserving scenario-reduction procedure applied to full 10000-scenario Monte Carlo ensembles
- a realistic Texas case study showing that seasonal joint outage spaces are line-dominated in failed-asset count but generator-sensitive in participation probability

The remainder of this paper is organized as follows. Section II presents the fragility-based seasonal outage modeling framework. Section III describes the probabilistic scenario generation and reduction methodology. Section IV reports the case-study results. Section V concludes the paper.

II. FRAGILITY-BASED SEASONAL OUTAGE MODELING

The proposed framework maps hurricane wind-gust data to bus-level outage probabilities for both transmission lines and generators, providing the probabilistic interface between hazard information and the stochastic outage scenarios developed in this work. Rather than relying on a small set of deterministic contingencies, it assigns wind exposure to each asset and translates that exposure into outage probability through asset-specific fragility representations, preserving heterogeneity in both hazard intensity and infrastructure vulnerability. The workflow consists of three steps: hazard assignment, fragility-based outage-probability estimation, and seasonal implementation.

A. Hazard Assignment to Transmission Lines and Generators

Wind data are derived from the ERA5 reanalysis [16], [17] and assigned to each bus connecting transmission lines and generators using proximity-based mapping. For each component, the nearest relevant weather station is identified, and its wind data are used as the representative hazard input. This preserves spatial variation in exposure without requiring continuous wind-field reconstruction at every asset location.

The reported case study uses maximum seasonal wind gust as the hazard variable. Maximum gust is included because short-duration wind peaks are strongly associated with structural loading and are commonly used in fragility-based outage modeling. Generator failure denotes direct wind-induced unavailability of the generating facility, not disconnection caused by a nearby line outage. For each asset, season, and hazard metric, the representative seasonal intensity is defined as the maximum wind exposure assigned to that asset over the corresponding seasonal record:

$$w_{i,q}^{m} = \max_{t \in T_q} w_{i,t}^{m} \tag{1}$$

where $w_{i,q}^{m}$ is the seasonal wind intensity assigned to asset i in season q under hazard metric m, $w_{i,t}^{m}$ is the wind exposure assigned to asset i at time t, and T_q is the set of time steps in season q. The metric index m is retained for generality; in the reported case study, m denotes maximum wind gust. This maximum-exposure representation is consistent with fragility-based wind-damage modeling because the most severe wind condition within the seasonal record governs the component outage probability.

B. Fragility-Based Outage Probability Estimation

The assigned seasonal wind intensity is converted into an outage probability using the asset-type-dependent lognormal fragility representation summarized in Table I [18], [19]:

$$p_k(w) = \Phi\left(\frac{\ln(w/\theta_k)}{\beta_k}\right) \tag{2}$$

where $p_k(w)$ is the outage probability of asset class k under wind intensity w, $\Phi(\cdot)$ is the standard normal cumulative distribution function, θ_k is the median wind intensity at which the damage probability equals 0.5, and β_k is the logarithmic dispersion parameter. In applying (2), w is replaced by the seasonal asset-level intensity $w_{i,q}^{m}$ from (1). This representation maps each assigned hurricane wind exposure to a continuous outage probability while allowing different asset classes to enter high-damage regimes at different wind-speed levels.

TABLE I
ASSET-SPECIFIC LOGNORMAL FRAGILITY PARAMETERS USED FOR HURRICANE WIND-DAMAGE MODELING.

Asset class k	θk (m/s)	βk
Distribution lines	58	0.28
Wind turbines	60	0.30
Distribution towers	62	0.28
Solar PV plants	63	0.32
Substations	66	0.35
Transmission lines	68	0.30
Battery storage plants	69	0.35
Nat. gas/oil/diesel/landfill gas plants	70	0.33
Coal and biomass power plants	72	0.30
Hydroelectric plants	75	0.30

The fragility coefficients in Table I are taken primarily from the EPRI infrastructure fragility-curve inventory [18], with the hurricane transmission-tower study in [19] supporting the transmission/tower parameterization. They are used as representative screening coefficients rather than event-calibrated estimates: θ_k denotes the 50% failure wind intensity, and β_k controls curve dispersion. Table I provides the exact coefficients, while Fig. 1 visualizes the resulting curve positions and slopes. Alternative-hazard and coefficient sensitivity are left for event-specific validation.

C. Seasonal Implementation

The framework is implemented on a seasonal basis using quarterly wind data from the ERA5 reanalysis [16], [17], because hurricane-related exposure and outage propensity are not temporally uniform. Hazard assignment and outage-probability estimation are repeated separately for each season, producing season-specific outage probabilities for both transmission lines and generators. Seasonality therefore enters before scenario generation, so that later outage ensembles reflect differences in underlying exposure and vulnerability rather than relying on post-hoc grouping.

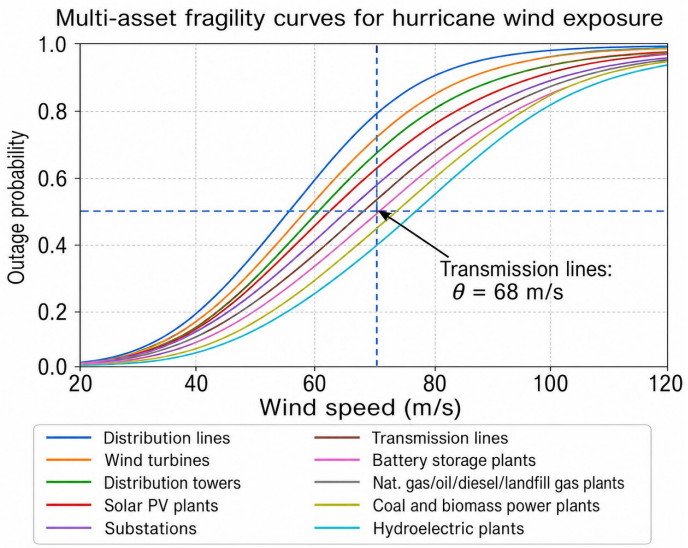

Fig. 1. Multi-asset fragility curves for hurricane wind exposure

III. PROBABILISTIC SCENARIO GENERATION AND REDUCTION

A. Full Scenario Construction

The component-level outage probabilities obtained in Section II are used to construct system-level stochastic outage scenarios. Three scenario sets are developed for transmission-only, generation-only, and joint transmission-generation outages, enabling analysis of the individual and combined effects of network-side and supply-side disruption within a common probabilistic framework.

For each outage class, a full Monte Carlo ensemble of 10000 scenarios is generated, where each scenario is a binary outage state over the relevant asset set. In each realization, a uniform random number is drawn for every represented component and compared with its fragility-derived outage probability through the Bernoulli state-generation rule:

$$x_{s,i} = \begin{cases} 0, & U_{s,i} < p_i, \\ 1, & U_{s,i} \geq p_i, \end{cases} \quad U_{s,i} \sim U(0,1) \tag{3}$$

where p_i is the fragility-derived outage probability of component i, and $U_{s,i}$ is an independent random draw for component i in scenario s. A state of 0 denotes a failed component and 1 an available one, consistent with the exported scenario-file convention of 0 = failed/unavailable and 1 = connected/available.

Because the complete binary outage space grows exponentially with the number of represented assets, exhaustive enumeration is impractical for a 9140-branch and 731-generator system; the 10000-scenario ensemble is therefore used as a statistically tractable approximation, with explicit scenario probabilities retained for later reduction. With 10000 trials, the worst-case 95% binomial confidence half-width is 0.0098. Analytical means check the sample; Monte Carlo retains compound and tail outage states and probability-bearing inputs for reduction that are unavailable from marginal probabilities.

The joint transmission-generation class combines the transmission-outage and generation-outage states into a single realization, so that later analysis reflects concurrent degradation of transfer capability and available supply. This construction is important because the outage structure induced by concurrent disruption is generally not recoverable from the isolated scenario classes alone.

B. Scenario Probability Representation

The scenario-probability formulation is retained explicitly for the three outage classes so that each Monte Carlo row is treated as a probability-bearing binary realization, not merely a list of failed components. For a line-only scenario, the probability of the exact realization is

$$\pi_s^L = \prod_{l \in \Omega_s^{L,F}} p_l \prod_{l \in \Omega_s^{L,A}} (1 - p_l) \tag{4}$$

where π_s^L is the probability of line-only scenario s, p_l is the fragility-derived outage probability of transmission line l, and $\Omega_s^{L,F}$ and $\Omega_s^{L,A}$ are the sets of failed and available transmission lines in scenario s. This is the transmission-line-only scenario-probability calculation used in earlier hurricane-resilience work [13].

For a generation-only scenario, the same formulation is applied to the generator asset set, and the exact realization probability is

$$\pi_s^G = \prod_{g \in \Omega_s^{G,F}} p_g \prod_{g \in \Omega_s^{G,A}} (1 - p_g) \tag{5}$$

where π_s^G is the probability of generation-only scenario s, p_g is the fragility-derived outage probability of generator g, and $\Omega_s^{G,F}$ and $\Omega_s^{G,A}$ are the sets of failed and available generators in scenario s. This mirrors the line-only expression, modeling generator outages with the same probability structure as transmission outages.

For the joint line-generator case, the same formulation is applied over the union of transmission-line and generator states. The combined failed set is $\Omega_s^F = \Omega_s^{L,F} \cup \Omega_s^{G,F}$, so a joint scenario may contain line failures, generator failures, or concurrent line-and-generator failures. The probability of the exact joint realization is

$$\pi_s^{LG} = \prod_{l \in \Omega_s^{L,F}} p_l \prod_{l \in \Omega_s^{L,A}} (1 - p_l) \prod_{g \in \Omega_s^{G,F}} p_g \prod_{g \in \Omega_s^{G,A}} (1 - p_g) \tag{6}$$

where l indexes transmission lines, g indexes generators, p_l and p_g are the fragility-derived outage probabilities of line l and generator g, and $\Omega_s^{L,F}$, $\Omega_s^{L,A}$, $\Omega_s^{G,F}$, and $\Omega_s^{G,A}$ denote the failed and available line and generator sets in scenario s. The union identifies the failed components, while the product gives the exact probability of the complete failed/available realization.

C. Representative Scenario Reduction

The full Monte Carlo ensembles are too large for direct downstream use, so they are reduced to smaller representative sets that preserve their dominant probabilistic structure. The generation-and-reduction sequence follows the established hurricane-resilience workflow [11]–[13], generalized here from the transmission-line-only formulation to the transmission-only, generation-only, and combined line-generator classes shown in Fig. 2. Although the procedure targets up to 50 representative scenarios, fewer may remain when the ensemble contains duplicate or near-duplicate outage states.

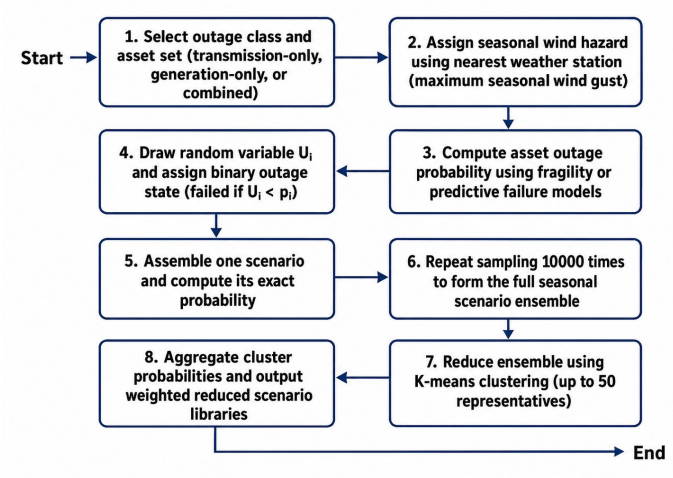

Fig. 2. Generalized workflow for probabilistic scenario generation and reduction under seasonal hurricane wind hazards

K-means is applied to the binary state vectors using squared Euclidean distance, equivalent to Hamming distance for binary entries. Up to 50 clusters are used, limited by distinct states, and the observed scenario nearest each centroid is retained. Scenario probabilities do not affect distance or assignment; after clustering, each representative receives the aggregate probability mass of its cluster. Therefore, the reduced-scenario probability is obtained by aggregating the probabilities of all full scenarios assigned to the corresponding cluster as follows.

$$\pi_r^{\text{red}} = \sum_{s \in C_r} \pi_s \tag{7}$$

where C_r is the set of full Monte Carlo scenarios assigned to reduced representative scenario r, which therefore carries the total probability mass of its cluster. This probability-preserving step is essential: without it, the reduced set would retain geometric representativeness but lose the probabilistic interpretation needed for consistent outage analysis. The reduced set size is thus an output of the scenario structure rather than a fixed parameter, in contrast with the rigid 50-scenario line-only presentation used in earlier transmission-only work [13].

IV. CASE STUDY AND RESULTS

A. Test System and Data

The proposed framework was demonstrated on the Texas 7k synthetic grid, a 6717-bus, 9140-branch, 731-generator test system on the geographic footprint of Texas built using the synthetic-grid construction methodology in [20], [21]. Wind exposure was derived from the ERA5 reanalysis [16], [17] and aggregated to seasonal maxima for each component, mapped to outage probabilities through (1), and used to generate 10000 Monte Carlo scenarios for each of the three outage classes. The ERA5-derived wind data used here are also available in the *.pww format in the Texas A&M University Electric Grid Test Case Repository [22], [23]. This section focuses on the statistical structure of the resulting outage space rather than downstream power-flow or restoration performance; the outputs should therefore be read as a transmission-line and generation-asset scenario library, with distribution, substation, and buried-line assets not treated as separate scenario-state variables.

B. Seasonal Outage Statistics

The mean failed-asset counts in Table II are validation summaries: their analytical values equal the sums of component outage probabilities, and the Monte Carlo estimates agree within sampling uncertainty. Transmission outages dominate the failed-asset count, with the fall season producing the largest mean line burden of 3591 failed lines, which is about 2.2 times the spring value and 2 times the summer value. Joint line-generator participation follows a different seasonal pattern: P(line and gen) is highest in spring and winter, reaching 0.87 and 0.71, respectively, but only 0.002 in summer and 0.047 in fall. Because at least one line outage occurs in every combined scenario, P(line and gen) equals the probability of any generator outage and therefore serves as the joint-participation metric for distinguishing seasonal line-generator structure. Table II summarizes these statistics for the full combined Monte Carlo scenario sets.

TABLE II
FULL COMBINED LINE-GENERATOR SCENARIO STATISTICS BY SEASON.

Season	P(line and gen)	Mean failed lines	Mean failed gens	Mean failed assets
spring	0.866	1624.83	1.98	1626.81
summer	0.002	1798.66	0.00	1798.66
fall	0.047	3590.58	0.05	3590.63
winter	0.708	2931.15	1.24	2932.39

Figure 3 visualizes this contrast: panel (a) reports the mean number of failed transmission lines by season, whereas panel (b) reports the probability that at least one generator fails in the combined scenario.

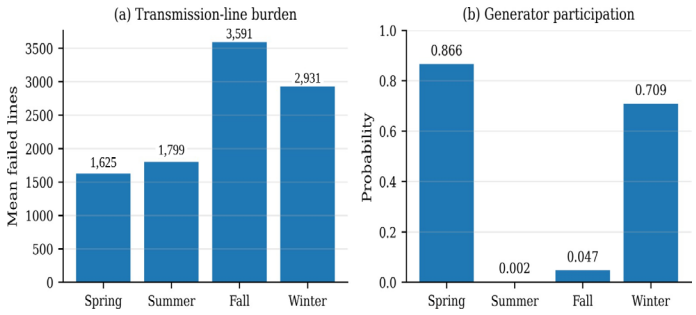

Fig. 3. Seasonal line burden and generator participation

C. Joint Outage Interpretation

Marginal probabilities provide expected counts but do not identify co-occurring line and generator failures. The combined class supplies compound states, showing spring/winter generator participation of 0.87/0.71 and yielding concurrent contingencies for downstream analysis. Fig. 4 links this pattern to seasonal exposure.

D. Hazard Exposure and Top-Risk Assets

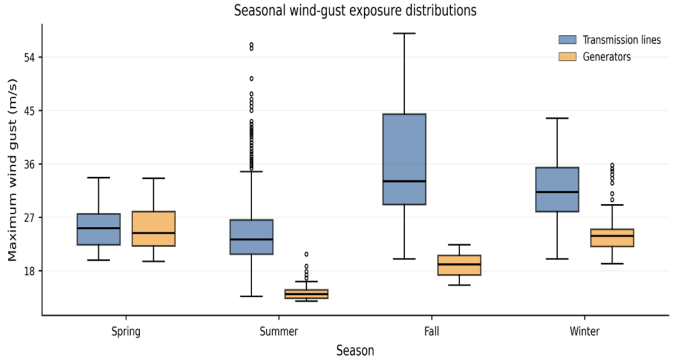

Fig. 4. Seasonal wind-gust exposure distributions in m/s

The hazard-side distributions in Fig. 4 are reported in m/s, consistent with the fragility parameters in Table I and the calculations in (2), and provide the physical explanation for the seasonal outage statistics. Transmission-line gust exposure reaches its highest median in fall at 33.1 m/s and remains elevated in winter at 31.3 m/s. Generator exposure follows a different pattern, with higher median gusts in spring and winter than in summer and fall. This mismatch between line-side and generator-side exposure explains why the combined scenario set is line-dominated in failed-asset count but generator-sensitive in participation probability.

Figure 5 directly reports component fragility probabilities: line risk is concentrated in summer/fall, while generator risk is strongest in spring/winter; it is not a Monte Carlo-specific statistic. These assets cluster within common Texas 7k bus areas, indicating spatially coherent network-and-supply exposure in the joint scenario library. Stratifying the generator-outage results by Texas 7k fuel type shows that generator risk is not fuel-type uniform: wind units dominate the spring generator-failure burden, while winter failures are

shared mainly between natural-gas and wind units. In capacity-weighted terms, wind units account for most expected failed generator capacity in spring and winter, whereas generator failures remain negligible in summer and small in fall. This structure helps explain why generator participation is seasonally selective even though the mean number of failed generators is small compared with the transmission-line burden.

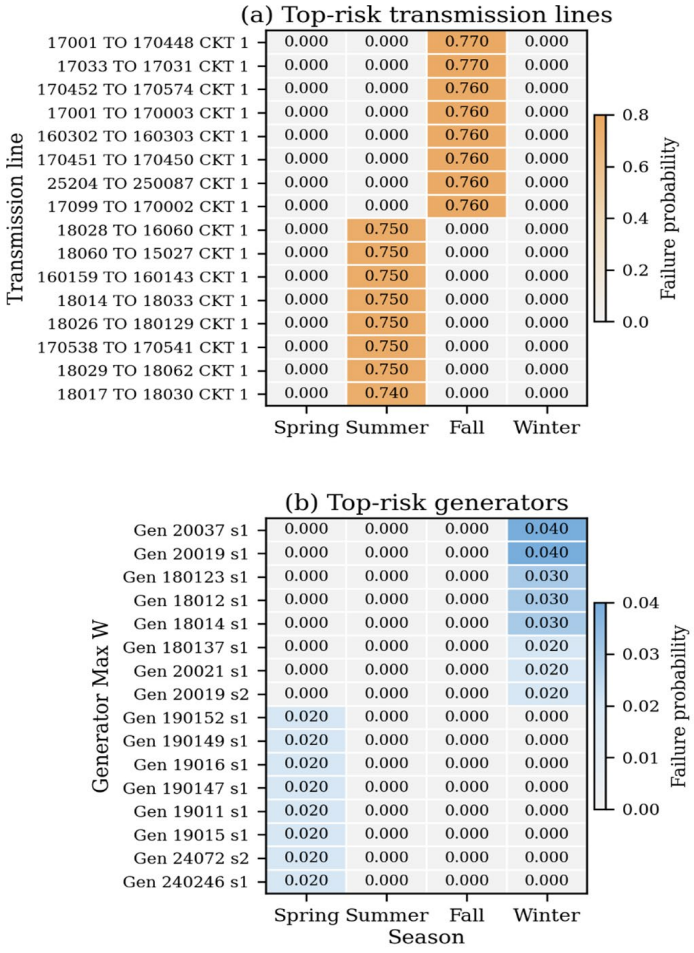

Fig. 5. Seasonal failure probabilities of selected top-risk assets in combined scenarios: (a) transmission lines and (b) generator units

E. Reduced Scenario Fidelity

The reduced scenario sets are evaluated by comparing probability-concentration metrics with full-versus-reduced fidelity for the combined line-generator scenarios.

Table III reports Monte Carlo-specific concentration and reduction fidelity: the mean failed-asset error remains within about 2.5%, summer reduces to nine scenarios with a top-1 probability of 0.999, and fall has a top-1 probability of 0.985. Here, Eff. scn. denotes the effective scenario count, computed from the normalized reduced-scenario probabilities as the inverse of their squared-probability sum; values near one indicate strong probability concentration, whereas larger values indicate greater effective scenario diversity. These quantities depend on compound-state frequencies and cluster assignments and cannot be obtained from marginal probabilities alone. Table IV reports the seasonal worst-case outage realization in terms of maximum failed assets.

TABLE III
REDUCED COMBINED LINE-GENERATOR SCENARIO CONCENTRATION AND FIDELITY BY SEASON.

Season	# scn.	Top 1	Top-5	Eff. scn.	Full mean Assets	Red. mean Assets	Error (%)
spring	50	0.590	0.669	2.83	1626.81	1621.46	−0.33
summer	9	0.999	1.000	1.00	1798.66	1841.89	2.40
fall	50	0.985	0.987	1.03	3590.63	3572.34	−0.51
winter	50	0.566	0.673	3.05	2932.39	2906.52	−0.88

TABLE IV
SEASONAL WORST-CASE OUTAGE REALIZATION (MAXIMUM FAILED ASSETS).

Season	spring	summer	fall	winter
Max assets	1754	1927	3759	3086

Taken together, the case-study results show that seasonal and joint outage modeling changes both the scale and the structure of the scenario space: the dominant numerical pattern is the large fall transmission burden, and the dominant joint-outage pattern is the high generator participation in spring and winter. These results justify retaining both the seasonal formulation and the explicit joint line-generator construction.

V. CONCLUSION

This paper presented a fragility-based seasonal framework for probabilistic outage scenario generation under hurricane wind hazards. We mapped component-level wind exposure to asset-dependent outage probabilities and generated seasonal transmission-only, generation-only, and joint line-generator scenario sets with explicit probabilities, reducing them to representative probability-weighted subsets. On the Texas 7k synthetic grid, the fall season produced the largest transmission outage burden, with 3591 mean failed lines, while spring and winter had the highest generator participation, reaching 0.87 and 0.71, respectively. The reduced sets preserved the dominant failed-asset burden and provide compact probability-weighted contingency libraries for downstream power-flow, restoration, and mitigation studies. Future work will extend the scenario library to well-documented Texas hurricane cases by incorporating storm duration, track/path characteristics, and occurrence frequency, and will couple the resulting probability-weighted outage scenarios with post-contingency analysis to evaluate line congestion, voltage-stability risk, emergency load shedding, controlled islanding, and mitigation strategies for cascading voltage collapse and severe operational stress.

REFERENCES

[1] H. Zhang, L. Cheng, S. Yao, T. Zhao, and P. Wang, "Spatial-temporal reliability and damage assessment of transmission networks under hurricanes," IEEE Transactions on Smart Grid, vol. 11, pp. 1044–1054, Mar. 2020.

[2] R. Nateghi, S. D. Guikema, and S. M. Quiring, "Forecasting hurricane-induced power outage durations," Natural Hazards, vol. 74, pp. 1795–1811, Dec. 2014.

[3] M. Panteli, C. Pickering, S. Wilkinson, R. Dawson, and P. Mancarella, "Power system resilience to extreme weather: Fragility modeling, probabilistic impact assessment, and adaptation measures," IEEE Transactions on Power Systems, vol. 32, pp. 3747–3757, Sep. 2017.

[4] M. Panteli, P. Mancarella, D. N. Trakas, E. Kyriakides, and N. D. Hatziargyriou, "Metrics and quantification of operational and infrastructure resilience in power systems," IEEE Transactions on Power Systems, vol. 32, pp. 4732–4742, Nov. 2017.

[5] O. S. Omogoye, K. A. Folly, and K. O. Awodele, "A review of power system predictive failure model for resilience enhancement against hurricane events," The Journal of Engineering, vol. 2021, no. 11, pp. 644–652, 2021.

[6] L. Xu, N. Lin, D. Xi, K. Feng, and H. V. Poor, "Hazard resistance-based spatiotemporal risk analysis for distribution network outages during hurricanes," IEEE Transactions on Power Systems, vol. 40, no. 3, pp. 2143–2152, 2025, doi: 10.1109/TPWRS.2024.3469168.

[7] L. Xu, N. Lin, D. Xi, K. Feng, and H. V. Poor, "Quantifying cascading power outages during climate extremes considering renewable energy integration," Nature Communications, vol. 16, p. 2435, 2025.

[8] F. Safdarian, J. Cook, K. Zhgun, T. J. Overbye, and J. Snodgrass, "Power flow modeling of the impacts of weather and other resiliency hazards with a focus on transmission planning," in Proceedings of the 58th Hawaii International Conference on System Sciences (HICSS), Waikoloa, HI, USA, Jan. 2025.

[9] T. J. Overbye, R. Badawi, S. G. Paal, and J. Snodgrass, "An extensible approach for modeling the impact of deterministic and stochastic external inputs in the power flow," in 2026 North American Power Symposium (NAPS), Houghton, MI, USA, Oct. 2026, to appear.

[10] L. Ceferino, N. Lin, and D. Xi, "Stochastic modeling of solar irradiance during hurricanes," Stochastic Environmental Research and Risk Assessment, vol. 36, pp. 2681–2693, Sep. 2022.

[11] N. Gröwe-Kuska, H. Heitsch, and W. Römisch, "Scenario reduction and scenario tree construction for power management problems," in 2003 IEEE Bologna Power Tech Conference Proceedings, vol. 3, Jun. 2003, p. 7 pp.

[12] Y. Zhuang, L. Cheng, N. Qi, M. R. Almassalkhi, and F. Liu, "Problem-driven scenario reduction framework for power system stochastic operation," IEEE Transactions on Power Systems, vol. 40, no. 4, pp. 3232–3246, Jul. 2025, doi: 10.1109/TPWRS.2024.3523220.

[13] M. Mahzarnia, M. P. Moghaddam, P. Siano, and M.-R. Haghifam, "A comprehensive assessment of power system resilience to a hurricane using a two-stage analytical approach incorporating risk-based index," Sustainable Energy Technologies and Assessments, vol. 42, p. 100831, 2020.

[14] A. Poudyal, A. Dubey, V. Iyengar, and D. Garcia-Camargo, "Spatiotemporal impact assessment of hurricanes on electric power systems," in 2022 North American Power Symposium (NAPS), Oct. 2022, pp. 1–6.

[15] P. KC, M. Naghibolhosseini, and M. Zayernouri, "Multi-scenario stochastic modeling of failure in power transmission lines," The Journal of Engineering, vol. 2025, no. 1, p. e70145, 2025.

[16] H. Hersbach, B. Bell, P. Berrisford et al., "The ERA5 global reanalysis," Quarterly Journal of the Royal Meteorological Society, vol. 146, pp. 1999–2049, Jul. 2020.

[17] "ERA5 hourly data on single levels from 1940 to present," [Online]. Available: https://doi.org/10.24381/cds.adbb2d47.

[18] Electric Power Research Institute (EPRI), "Fragility curve inventory," [Online], 2024, available: https://apps.epri.com/ climate-vulnerabilities-adaptations/en/fragility.html.

[19] X. Du and J. F. Hajjar, "Methodology for collapse fragility development for hurricane events: Electrical transmission towers," Journal of Constructional Steel Research, vol. 223, p. 109005, 2024.

[20] A. B. Birchfield, T. Xu, K. M. Gegner, K. S. Shetye, and T. J. Overbye, "Grid structural characteristics as validation criteria for synthetic networks," IEEE Transactions on Power Systems, vol. 32, pp. 3258–3265, Jul. 2017.

[21] A. B. Birchfield, T. Xu, and T. J. Overbye, "Power flow convergence and reactive power planning in the creation of large synthetic grids," IEEE Transactions on Power Systems, vol. 33, pp. 6667–6674, Nov. 2018.

[22] S. Kunkolienkar, F. Safdarian, J. Snodgrass, A. Birchfield, and T. Overbye, "A description of the Texas A&M university electric grid test case repository for power system studies," in 2024 IEEE Texas Power and Energy Conference (TPEC), College Station, TX, USA, Feb. 2024.

[23] Texas A&M University, "Texas A&M university electric grid test case repository," [Online], available: https://electricgrids.engr.tamu.edu.